Analytica Chimica Acta 696 (2011) 116–124

Contents lists available at ScienceDirect

Analytica Chimica Acta

journal homepage: www.elsevier.com/locate/aca

# A stepwise strategy employing automated screening and DryLab modeling for the development of robust methods for challenging high performance liquid chromatography separations: A case study

K. Jayaraman, A.J. Alexander*, Y. Hu, F.P. Tomasella

*Analytical & Bioanalytical Development, Bristol - Myers Squibb Company, 1 Squibb Drive, New Brunswick, NJ 08903, USA*

ARTICLE INFO

*Article history:*
Received 22 December 2010
Received in revised form 30 March 2011
Accepted 9 April 2011
Available online 16 April 2011

*Keywords:*
Method development strategy
Column screening system
Method optimization
DryLab®

ABSTRACT

A stepwise method development strategy has been employed to develop a robust HPLC method to resolve several closely eluting structurally related impurities in an active pharmaceutical ingredient (API). This strategy consisted of automated column screening, optimization of the most critical chromatographic parameters, DryLab® modeling, and experimental verification of optimized separation conditions. DryLab® was used to predict an optimized gradient profile and separation temperature and these predictions were verified experimentally. A discussion of the accuracy of these predictions is presented. The robustness of the method was verified and the ability of DryLab® to predict, with reasonable accuracy, the outcome of such robustness studies was also examined. Once the robustness was established by the DryLab® predictions the remainder of the subsequent verification by experiment becomes a simple reiterative exercise. This study also demonstrates that factors such as column chemistry and critical chromatographic parameters can have a profound and oftentimes interrelated effect on the chromatographic separation of isomers, bromo analogs and other structurally very similar impurities. Therefore, it is critical to adopt a rational strategy, as demonstrated here, to evaluate the interplay of these factors, thereby greatly enhancing method development efficiency.



## 1. Introduction

High performance liquid chromatography (HPLC) method development by the conventional trial-and-error methodology is no longer an effective practice in the pharmaceutical industry. Changing only one variable at a time is labor intensive and time consuming and involves intensive exploitation of equipment and a substantial consumption of solvents [1]. The objective of automated method development is not only to reduce this trial-and-error factor in the optimization of complex separations [1], but also to provide automated control of the instrumentation, column selection, mobile phase choice, and other experimental parameters [2]. Several stand alone HPLC method development software packages are now commercially available and the use of such programs for the computer-assisted optimization of liquid chromatography separations of drugs and related substances has been reviewed [1]. Krisko et al. [3] described the application of an automated column selection system using a series of HPLC columns, in combination with DryLab® software (Molnar-Institut fur Angewandte Chromatographie, Berlin, Germany) to efficiently develop HPLC methods. More recently, Corredor et al. [4] demonstrated a comprehensive, two-phase strategy for the development of a reversed-phase HPLC–UV chromatographic method for a basic drug candidate. Phase 1 of the strategy employed an automated column selection system and solvent screening. In phase 2, DryLab® software was used to establish the optimal operating conditions. The historical mile stones and concepts associated with the development of this software were reviewed by Molnar in 2002 [5]. Having initially conducted a small well-defined number of experiments on a particular stationary phase, DryLab® can be used to predict the separation following changes in mobile phase composition, mode of elution (either isocratic or gradient), temperature, pH or column parameters (dimensions, particle size, flow rate) [4,5]. Dolan et al. showed that four experimental runs, where both temperature $T$ and gradient time $t_G$ are varied, were sufficient for the reliable DryLab® computer prediction of separation as a function of these two variables (two-dimensional optimization) [6]. Under these conditions Dolan et al. also examined the simulation errors that can arise from inexact expressions for retention time as a function of $T$, $t_G$ or isocratic %B. [7]. They concluded that, for the case where gradient separations were predicted on the basis of initial (input) gradient runs (and $T$ is constant), the average error in resolution (Rs) was in most cases <0.2 units for all samples (i.e., acceptable). Furthermore, for gradient predictions where

* Corresponding author. Tel.: +1 7322276737.
*E-mail address:* Anthony.Alexander@bms.com (A.J. Alexander).

0003-2670/$ – see front matter © 2011 Elsevier B.V. All rights reserved.
doi:10.1016/j.aca.2011.04.010

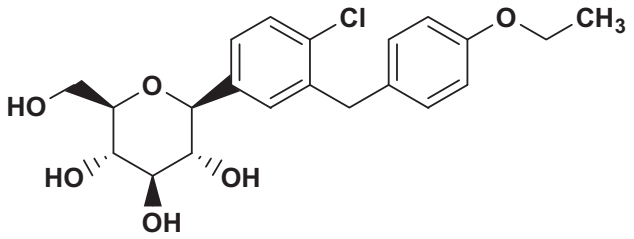


**Fig. 1.** Structure of Dapagliflozin, CAS: 461432-26-8.

$T$ also varies, the average error in resolution was also found to be acceptable for most samples. Exceptions to these conclusions were noted for samples (a) composed of molecules of quite different shape and (b) containing partially ionized acids or bases. For such samples, retention as a function of temperature is less predictive, and predictive errors can be quite large when a wide range in $T$ ($\Delta T > 20\,^{\circ}C$) is explored. Similar levels of predictive accuracy for DryLab® have been reported more recently by Fekete et al. [8] in a study utilizing fast liquid chromatography with 5 cm long narrow bore columns packed with sub-2 μm particles. Under these conditions the authors reported Rs errors ranging from −2.89% to −1.64% for an isocratic %B-temperature model and from −5.56% to 4.97% for a gradient time-mobile phase pH model respectively.

Method development software is becoming more sophisticated and integrated with all aspects of the chromatographic separation. Thus, most of the strategies described in the literature [2–4,9–11] involve all, or most of, the following steps: (1) automated column and mobile phase screening, (2) selection of column and mobile phase compositions based on the automated screening results and (3) computer assisted optimization using the selected column and mobile phase compositions. The automated multicolumn screening system used in this work (MeDuSA [12]) was employed to screen for differences in stationary phase selectivity, as well as organic modifier, thus allowing the primary separation parameters to be rapidly established. One improvement to this development strategy would be to include a step that involves experimental scouting of the critical chromatographic parameters after column screening and prior to software optimization. Also, the use of DryLab® could be extended to include the evaluation of method robustness studies. In this work we describe a step-wise strategy for pharmaceutical method development which incorporates these innovations, that is: (a) automated column screening, (b) experimental scouting of the critical chromatographic parameters (c) DryLab® optimization of the method, (d) experimental verification of the optimized conditions and (e) method robustness studies employing DryLab® which can be used as a predictive tool prior to validation and (f) the validation of the finalized method.

The development of the impurity profiling and assay method described in this paper was particularly challenging as the potential impurities present in the sample were structurally very similar to the API itself. That is, the sample consisted of the API, which in this case is Dapagliflozin (see Fig. 1 for structure), the bromo-analog of the API (B), the (-isomer of the API (C), the regio-isomer of the bromo analog (A) and an –OMe process related impurity (D). The development of Dapagliflozin, which includes details of the synthesis, has recently been reviewed by Cole et al. [13].

## 2. Experimental

### 2.1. Chemicals

Dapagliflozin [13] and its isomers were provided by the Process Research and Development in Bristol-Myers Squibb, New Brunswick, NJ. All HPLC grade solvents were obtained from J.T. Baker (Mallinckrodt Baker, Inc. Phillipsburg, NJ, USA). Water (18.2 MΩ cm) was obtained using an in-house Milli-Q system (Millipore, Billerica, MA, USA). An impurity marker solution was prepared from the individual components such that the API was present at a concentration of 0.2 mg $mL^{-1}$ and the other compounds (A–D) were present at approximately 0.4–1.1 area% relative to the API. Acetonitrile was used as the sample diluent.

### 2.2. HPLC columns

The HPLC columns listed in Table 1 and used in this study were purchased from the respective vendors.

### 2.3. Instrumentation and software

Automated column screening experiments were performed using a multidimensional screening analysis (MeDuSA) system based on Shimadzu Vp hardware and software (Shimadzu Scientific Instruments, Inc). A detailed description of this system has been previously published [12] and will not be discussed in detail here. Other chromatographic evaluation and measurements were made on a Waters (Milford, MA, USA) 2695 Alliance HPLC system equipped with a Waters 2487 detector and a Hewlett-Packard (Palo Alto, CA, USA) 1100 system equipped with a diode array detector. Waters Empower Software (Feature Release 2) was used to acquire, store and process the chromatographic data. Retention times and peak areas of individual peaks from experimental runs were used as input data for DryLab® Chromatography Optimization Software (Molnar Institut, Berlin, Germany).

## 3. Results and discussion

### 3.1. Initial method development strategy

Prior to the start of this work it was not possible to separate the bromo API analog (B) from the α-isomer (C) of the API, or separate the regio-isomer of the bromo analog (A) from the API using an existing method (YMC Pro C18 column). Hence, as this compound entered the development pipeline, it was necessary to develop a method that could separate API, A, B, C and D (a process impurity) from each other. From examination of the chemical structures of the API, A, B, C and D, it was concluded that they do not have any ionisable groups and hence varying mobile phase pH, or ionic strength, will not yield any significantly improvement in separation between these species (also experimentally confirmed below). This effectively limits the utilizable chromatographic parameters to temperature, solvent strength and gradient time ($t_G$).

Therefore, the HPLC method development was focused towards achieving selectivity through the identification of a suitable stationary phase, selecting a practical organic modifier and separation temperature and finally performing software assisted fine optimization of the selected method. Compounds B and C are the critical pair in this separation and the initial focus of the method development optimization was to effectively separate these species. In addition, a reduction in run time is desirable. Finally, since the impurities in question are at low levels, approximately 0.1%, any changes in the method parameters should have no negative impact on the peak shape (tailing) of the API and all the low level impurities.

### 3.2. Automated column screening and column selection

Using the MeDuSA system, the impurity marker mixture sample was screened using a selected set of columns given in Table 1. These columns were selected to reveal conditions that might provide improved resolution, selectivity, and peak shape all within an acceptable run time. The columns were selected based on the column comparison function F derived from the USP-PQRI web

**Table 1**
HPLC columns used in the MeDuSA column screening process.

| *F* value[a] | Column name[b] | Description |
|---|---|---|
| 8.9 | Phenomenex Synergi Hydro-RP (1) | High efficiency silica, C18 with polar end capping |
| 0 | YMC Pro C18 (2) | C18 bonded to ultra pure silica with Lewis acid–base end capping |
| 4.3 | Phenomenex Luna C8 (3) | Luna Silica, C8, endcapped |
| 4.6 | Waters Symmetry Shield RP-8 (4) | C8 with embedded polar group |
| 12.7 | Waters XTerra RP18 (5) | C18, bonded and end capped Xterra particle, Hybrid Particle Technology, embedded polar group |
| 5.2 | Phenomenex Luna C5 (6) | Luna Silica, C5, end capped |
| 3.7 | Phenomenex Synergi Max – RP (7) | High efficiency silica, C12, TMS end capping |
| 12.5 | Waters XTerra Phenyl (8) | Combination of Hybrid Particle Technology and Xterra Phenyl chemistry, difunctional bonding |
| 4.8 | YMC Pack Pro C18 RS (9) | C18 with polymeric bonding to ultra pure silica with Lewis acid–base end capping |
| 5.9 | Waters XTerra MS C8 (10) | C8, tri-functional bonding chemistry, embedded polar group |
| 10.7 | Thermo Hypersil Gold (11) | Ultra-pure Silica, C18, end capped |
| 5.7 | Phenomenex Synergi Fusion-RP (12) | High efficiency silica, C18 with polar embedding |
| 5.5 | Zorbax Extend C18 (13) | C18, unique patented bidentate silane, combined with double end capping |
| 5.9 | Waters XBridge C8 (14) | XBridge particle, C8, trifunctional bonding, end capped |
| 5.31 | Waters Sunfire C18 (15) | State-of-the-art reversed phase C18 bonded silica, new bonding and end capping |
| 10.7 | Thermo Hypersil Gold PFP (16) | Ultra-pure Silica, pentafluorophenyl ligand, endcapped |
| 12.2 | Waters XBridge Phenyl (17) | XBridge particle, C6 phenyl, trifunctional bonding, end capped |
| 5.0 | Phenomenex Gemini C18 (18) | Unique silica organic layer, C18 with TMS end capping |
| 8.8 | Waters Xbridge Shield RP18 (19) | XBridge particle, C18, patented monofunctional silane with embedded polar carbamate group |

[a] Column comparison function *F* derived from the USP-PQRI web calculator [14] using YMC Pro C18 as the evaluation column. Values of $F > 3$ indicate columns of different selectivity.
[b] Number in parenthesis after column description is the designated column number, 1–19.

calculator [14,15] which, in-turn, is based on the hydrophobic-subtraction model of reverse-phase column selectivity [16]. Using this calculator, values of $F > 3$ can be used to select columns of different selectivity. In this case, the column selected for comparison to the PQRI database was the one used in the original method, that is, a YMC Pro C18 column. Values of *F* for the columns selected for screening ranged between 3.7 (Phenomenex Synergi Max-RP) and 12.5 (Waters Xterra Phenyl). Table 2 lists the selected mobile phase and HPLC conditions. All 19 columns listed in Table 1 were evaluated using the eluents (A1, B1), (A2, B2) and (A4, B4) listed in Table 2. All columns except 1, 2, 4, 15 and 16 were also evaluated using the eluents (A3, B3). Single wavelength UV detection was performed at 220 nm and the injection volume was set at 10 μL.

### 3.3. Experimental scouting of the critical chromatographic parameters

#### 3.3.1. Organic modifier selection

The most promising MeDuSA separations were obtained with XBridge Shield RP18 ($F = 8.8$) and Sunfire C18 ($F = 5.3$) columns and hence these stationary phases were selected for further method development. The selection of these column chemistries was based on the number of peaks detected, and the separation of the critical peaks (B and C). Interestingly, the separations obtained from columns with significantly higher *F* values, and thus greater potential for orthogonality, such as Waters XTerra Phenyl ($F = 12.5$) and Thermo Hypersil Gold PFP ($F = 10.7$) were less promising. Organic modifier screening was then performed on the XBridge Shield RP18 and Sunfire C18 columns to evaluate the ability of the method to separate API, A, B, C and D from each other. Table 3 lists the organic modifiers and the gradients employed together with applicable method parameters. Note that the sample mixture contained all the components at different ratios for easy peak identification. Fig. 2 illustrates the chromatographic resolution as a function of the type of organic modifier employed for the XBridge column. With this column, peaks A and B are poorly separated in the acetonitrile based mobile phase while they are better separated in the mobile phase containing methanol. Fig. 3 illustrates the same comparison for the Sunfire column. In this case peaks B and C are poorly separated using methanol while they are well separated in the acetonitrile based mobile phase. It is interesting to note that the selectivity difference exhibited by the two organic modifiers (ACN versus MeOH) is greater for peaks A and B with the XBridge column while it is greater for peaks B and C with the Sunfire column. When THF was employed as the organic modifier the separation of component A from the API was increased for both the Sunfire and XBridge columns, however, the poorer resolution obtained between components A, B, C and D, indicated that no significant selectivity advantage could be gained from using this solvent with either column. Thus, the XBridge column, with methanol as organic modifier and the Sunfire column, with acetonitrile as organic modifier, were selected for further method development studies.

**Table 2**
HPLC conditions for the column screening analysis.

| | |
|---|---|
| Eluents | pH = 2<br>A1 = 0.05% TFA in $CH_3OH$:$H_2O$ (20:80)<br>B1 = 0.05% TFA in $CH_3OH$:$CH_3CN$ (20:80)<br>pH = 7<br>A2 = 0.01 M $NH_4OAc$ in $CH_3OH$:$H_2O$ (20:80)<br>B2 = 0.01 M $NH_4OAc$ in $CH_3OH$:$H_2O$:$CH_3CN$ (20:5:75)<br>pH = 9<br>A3 = 0.05% $NH_4OH$ in $CH_3OH$:$H_2O$ (20:80)<br>B3 = 0.05% $NH_4OH$ in $CH_3OH$:$CH_3CN$ (20:80)<br>pH = 2<br>A4 = 0.05% TFA in $CH_3CN$:$H_2O$ (10:90)<br>B4 = 0.05% TFA in $CH_3CN$<br>*Note: no MeOH in either mobile phase A4 or B4* |
| Gradient | 10%B to 100%B in 35 min |
| Flow rate (mL $min^{-1}$) | 1.0 |
| Wavelength (nm) | 220 |

**Table 3**
HPLC conditions for organic modifier screening analysis.

| | |
|---|---|
| Organic modifiers | Pair 1:<br>0.05% TFA in 100% $H_2O$<br>0.05% TFA in 100% $CH_3CN$<br>Pair 2:<br>0.05% TFA in $CH_3OH$:$H_2O$ (20:80)<br>0.05% TFA in $CH_3OH$:$CH_3CN$ (20:80)<br>Pair 3:<br>0.05% TFA in 100% $H_2O$<br>0.05% TFA in THF:$CH_3CN$ (40:60) |
| Gradient | Pairs 1 and 2:<br>15–100%B in 35 min<br>Pair 3: 12.8–85.4%B in 35 min |

*Note*: See Table 2 for mobile phase flow rate and UV wavelength values.

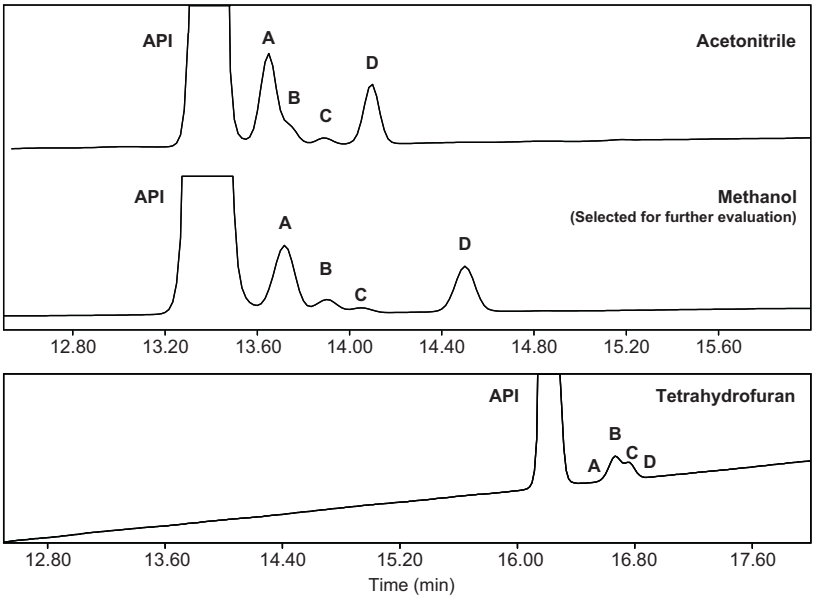


**Fig. 2.** Influence of the organic modifier on the separation of Dapagliflozin impurity marker components using an XBridge Shield RP18 column. Acetonitrile, methanol and tetrahydrofuran were selected as organic modifiers. See Table 3 for other method conditions employed. Peak identities ordered by increasing retention time are: API, Dapagliflozin; A, regio-isomer of the API bromine analog; B, bromine-analog of the API; C, (-isomer of the API; D, –OMe process related impurity of API.

*3.3.2. Separation temperature evaluation*

As the separation efficiency and selectivity in HPLC is often temperature dependent [17], both the XBridge and Sunfire columns were evaluated over a temperature range of 15–35 °C. Mobile phase pairs 1 and 2, described in Table 3, were used for the Sunfire and XBridge columns respectively. Three different temperatures (15 °C, 25 °C and 35 °C) were evaluated with a gradient of 15–100%B in 35 min. A flow rate of 1 mL min$^{-1}$ and a wavelength of 220 nm were used. Fig. 4 and Fig. 5 illustrate the effect of column temperature on the separations obtained with the XBridge and Sunfire columns respectively. The separation on the XBridge column exhibited negative temperature dependence; with the best resolution being obtained at 15 °C, whereas, the separation on the Sunfire column exhibited positive temperature dependence; with temperatures of 25 °C and 35 °C both yielding the best separation efficiency.

*3.4. Selection of column and organic modifier*

Results from the initial screening experiments indicated that a Sunfire C18 column, with acetonitrile as modifier and operated within a temperature range of 25–35 °C provided good resolution of critical pairs. Hence this combination of column and organic modifier was selected as a basis for DryLab® software optimization of

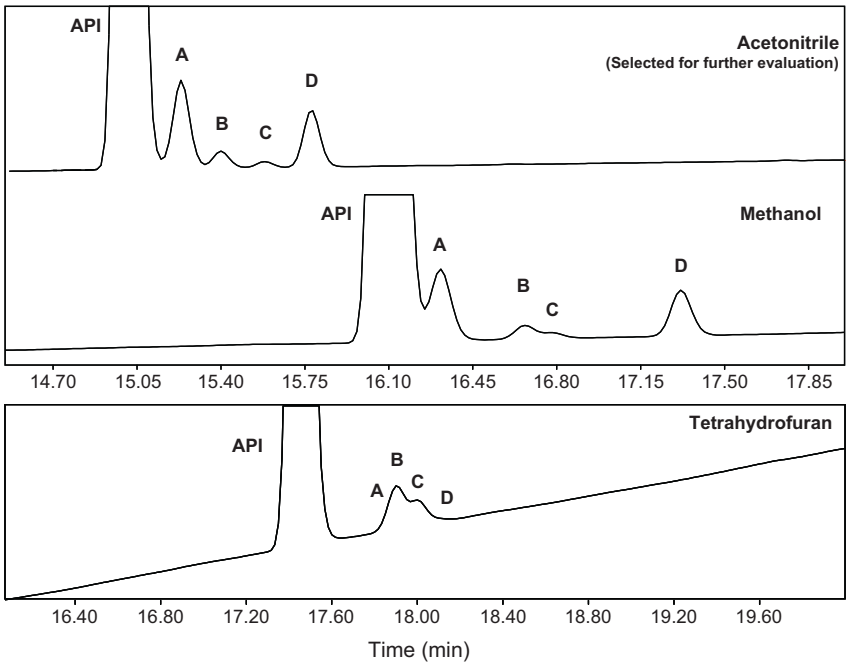


**Fig. 3.** Influence of the organic modifier on the separation of Dapagliflozin impurity marker components using a Sunfire C18 column. Acetonitrile, methanol and tetrahydrofuran were selected as organic modifiers. See Table 3 for other method conditions employed.

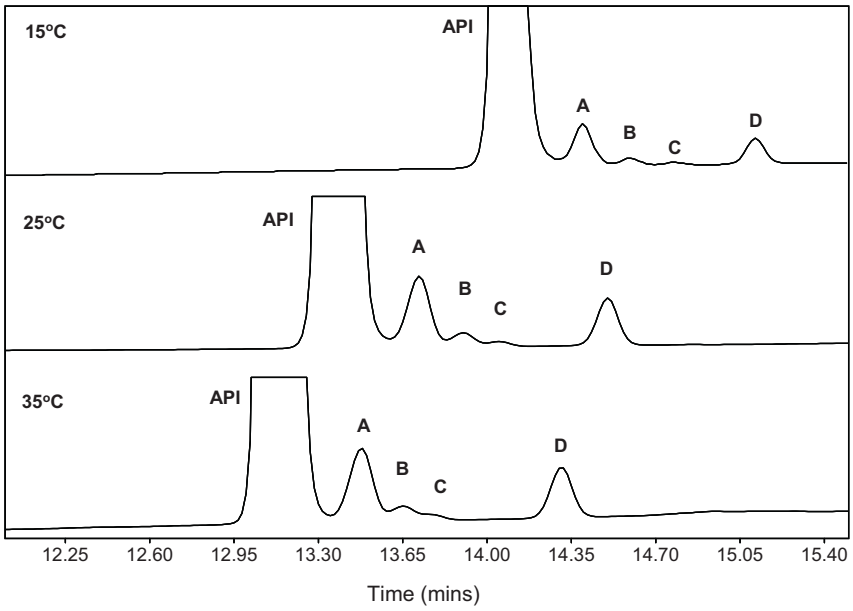


**Fig. 4.** Influence of column temperature on the separation of Dapagliflozin impurity marker components using an XBridge Shield RP18 column. Selected temperatures: 15 °C, 25 °C, and 35 °C. See Table 3 for other method conditions employed.

the method. It should be noted that, although a comparable separation could be obtained from a combination of an Xbridge Shield RP18 column, with methanol as modifier at a temperature of 15 °C, this combination was considered to be less robust for the following reasons: (a) acetonitrile offers lower UV background and lower back-pressure as compared to methanol and (b) a separation temperature of 30 ± 5 °C is easier to control than 15 °C for most HPLC systems.

### 3.5. Optimization of selected method conditions using DryLab®

DryLab® can be employed to model either one or two variables [5,10]. In this work we choose the two variable LC–RP Gradient/Temperature mode to predict the optimized conditions. Using the Sunfire column and acetonitrile modifier combination, the following chromatographic separations were performed: *Run 1*: 20-min gradient at 25 °C, *Run 2*: 60-min gradient at 25 °C, *Run 3*: 20-min gradient at 45 °C and *Run 4*: 60-min gradient at 45 °C (see Table 4 column 2). These four runs were chosen based on the following considerations: (a) gradient times should differ by a factor of 3–4 for DryLab® predictions and the optimized gradient time should be between 20 and 60 min, (b) the Sunfire column was found to perform better at temperatures of ≥25 °C and the $\Delta T$ recommendation for DryLab® is 20 °C, hence a temperature range of 25–45 °C were chosen for input data and (c) a wide gradient range of 5–100%B was chosen for all four runs so a broad design space could be modeled by DryLab®. In this manner the full depth and breadth of the design space would be explored, compared to

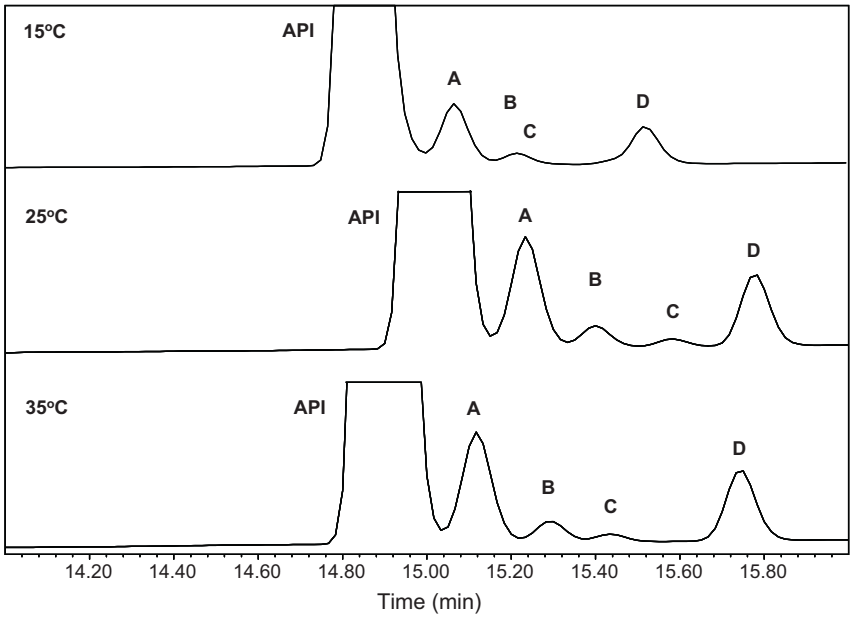


**Fig. 5.** Influence of column temperature on the separation of Dapagliflozin impurity marker components using a Sunfire C18 column. Selected temperatures: 15 °C, 25 °C, and 35 °C. See Table 3 for other method conditions employed.

**Table 4**
DryLab® input conditions and final HPLC conditions.

| | DryLab® input conditions | Final condition |
|---|---|---|
| Column | Sunfire C18, 4.6 mm × 150 mm, 3.5 μm | |
| Mobile phase | A: 0.05% TFA in water<br>B: 0.05% TFA in acetonitrile | |
| Column temperature (°C) | 25 and 45 | 30 |
| Wavelength (nm) | 220 | |
| Flow rate (mL min$^{-1}$) | 1.0 | |
| Gradient | 5–100%B in 20 min<br>5–100%B in 60 min | 15–90%B in 34 min |

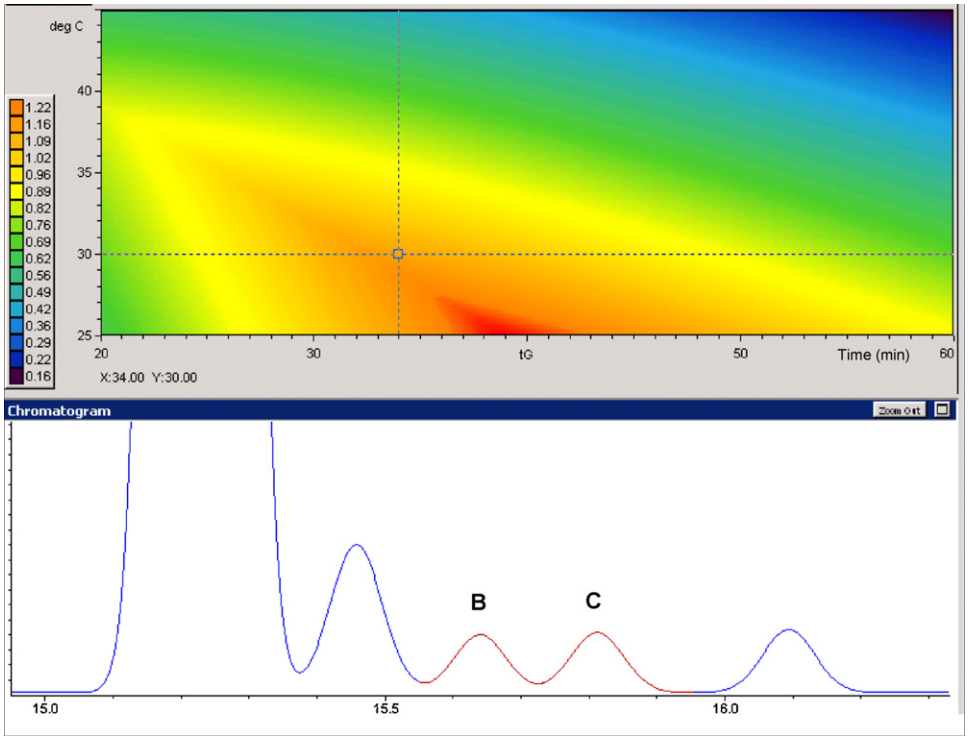


**Fig. 6.** DryLab® resolution map obtained for the separation of Dapagliflozin impurity marker components obtained using the LC–RP Gradient/Temperature mode to predict the optimized separation conditions (see Section 3.5).

Retention Time (min)

Column Temperature (°C)

| | 25.0 | 26.0 | 27.0 | 28.0 | 29.0 | 30.0 | 31.0 | 32.0 | 33.0 | 34.0 | 35.0 | 36.0 | 37.0 | 38.0 | 39.0 | 40.0 | 41.0 | 42.0 | 43.0 |
|---|---|---|---|---|---|---|---|---|---|---|---|---|---|---|---|---|---|---|---|
| 35.0 | 0.98 (2,3) | 1.00 (3,4) | 0.99 (3,4) | 0.98 (3,4) | 0.97 (3,4) | 0.95 (3,4) | 0.94 (3,4) | 0.93 (3,4) | 0.92 (3,4) | 0.90 (3,4) | 0.89 (3,4) | 0.88 (3,4) | 0.86 (3,4) | 0.85 (3,4) | 0.83 (3,4) | 0.82 (3,4) | 0.80 (3,4) | 0.79 (3,4) | 0.77 (3,4) |
| 34.0 | 0.96 (2,3) | 1.00 (2,3) | 1.03 (3,4) | 1.02 (3,4) | 1.01 (3,4) | 1.00 (3,4) | 0.99 (3,4) | 0.98 (3,4) | 0.96 (3,4) | 0.95 (3,4) | 0.94 (3,4) | 0.92 (3,4) | 0.91 (3,4) | 0.89 (3,4) | 0.88 (3,4) | 0.86 (3,4) | 0.85 (3,4) | 0.83 (3,4) | 0.81 (3,4) |
| 33.0 | 0.95 (2,3) | 0.99 (2,3) | 1.02 (2,3) | 1.05 (2,3) | 1.06 (3,4) | 1.05 (3,4) | 1.03 (3,4) | 1.02 (3,4) | 1.01 (3,4) | 0.99 (3,4) | 0.98 (3,4) | 0.97 (3,4) | 0.95 (3,4) | 0.94 (3,4) | 0.92 (3,4) | 0.91 (3,4) | 0.89 (3,4) | 0.88 (3,4) | 0.86 (3,4) |
| 32.0 | 0.94 (2,3) | 0.97 (2,3) | 1.01 (2,3) | 1.04 (2,3) | 1.07 (2,3) | 1.09 (3,4) | 1.08 (3,4) | 1.07 (3,4) | 1.05 (3,4) | 1.04 (3,4) | 1.03 (3,4) | 1.01 (3,4) | 1.00 (3,4) | 0.98 (3,4) | 0.97 (3,4) | 0.95 (3,4) | 0.94 (3,4) | 0.92 (3,4) | 0.90 (3,4) |
| 31.0 | 0.92 (2,3) | 0.96 (2,3) | 0.99 (2,3) | 1.03 (2,3) | 1.06 (2,3) | 1.09 (2,3) | 1.13 (3,4) | 1.11 (3,4) | 1.10 (3,4) | 1.09 (3,4) | 1.07 (3,4) | 1.06 (3,4) | 1.04 (3,4) | 1.03 (3,4) | 1.01 (3,4) | 0.99 (3,4) | 0.98 (3,4) | 0.96 (3,4) | 0.95 (3,4) |
| 30.0 | 0.91 (2,3) | 0.94 (2,3) | 0.98 (2,3) | 1.01 (2,3) | 1.05 (2,3) | 1.08 (2,3) | 1.11 (2,3) | 1.15 (2,3) | 1.15 (3,4) | 1.13 (3,4) | 1.12 (3,4) | 1.10 (3,4) | 1.09 (3,4) | 1.07 (3,4) | 1.06 (3,4) | 1.04 (3,4) | 1.02 (3,4) | 1.01 (3,4) | 0.99 (3,4) |
| 29.0 | 0.89 (2,3) | 0.93 (2,3) | 0.96 (2,3) | 1.00 (2,3) | 1.03 (2,3) | 1.07 (2,3) | 1.10 (2,3) | 1.13 (2,3) | 1.17 (2,3) | 1.18 (3,4) | 1.16 (3,4) | 1.15 (3,4) | 1.13 (3,4) | 1.12 (3,4) | 1.10 (3,4) | 1.08 (3,4) | 1.07 (3,4) | 1.05 (3,4) | 1.03 (3,4) |
| 28.0 | 0.88 (2,3) | 0.91 (2,3) | 0.95 (2,3) | 0.98 (2,3) | 1.02 (2,3) | 1.05 (2,3) | 1.09 (2,3) | 1.12 (2,3) | 1.15 (2,3) | 1.19 (2,3) | 1.21 (3,4) | 1.20 (3,4) | 1.18 (3,4) | 1.16 (3,4) | 1.15 (3,4) | 1.13 (3,4) | 1.11 (3,4) | 1.10 (3,4) | 1.08 (3,4) |
| 27.0 | 0.86 (2,3) | 0.90 (2,3) | 0.94 (2,3) | 0.97 (2,3) | 1.01 (2,3) | 1.04 (2,3) | 1.07 (2,3) | 1.11 (2,3) | 1.14 (2,3) | 1.17 (2,3) | 1.20 (2,3) | 1.24 (2,3) | 1.23 (3,4) | 1.21 (3,4) | 1.19 (3,4) | 1.18 (3,4) | 1.16 (3,4) | 1.14 (3,4) | 1.12 (3,4) |
| 26.0 | 0.85 (2,3) | 0.89 (2,3) | 0.92 (2,3) | 0.96 (2,3) | 0.99 (2,3) | 1.03 (2,3) | 1.06 (2,3) | 1.09 (2,3) | 1.13 (2,3) | 1.16 (2,3) | 1.19 (2,3) | 1.22 (2,3) | 1.25 (2,3) | 1.25 (3,4) | 1.24 (3,4) | 1.22 (3,4) | 1.21 (3,4) | 1.19 (3,4) | 1.17 (3,4) |

**Fig. 7.** DryLab® resolution table obtained for separation of Dapagliflozin impurity marker components obtained using the LC–RP Gradient/Temperature mode to predict the optimized separation conditions (see Section 3.5).

**Table 5**
DryLab® predicted and experimental value for the resolution and retention time.

| Peak identity | Retention time (min) | | | | | Resolution (Rs) | | | | |
|---|---|---|---|---|---|---|---|---|---|---|
| | Predicted[a] | Experimental results | Av. exp. | Diff[b] | % error[c] | Predicted[a] | Experimental results | Av. exp. | Diff.[b] | % Error[c] |
| API | 15.23 | 15.29,15.26,15.27,15.28 | 15.28 | 0.05 | 0.33 | NA | NA | NA | NA | NA |
| A | 15.46 | 15.52,15.48,15.49,15.50 | 15.50 | 0.04 | 0.26 | 1.60 | 1.61,1.60,1.61,1.60 | 1.60 | 0.1 | 6.67 |
| B | 15.64 | 15.71,15.68,15.69,15.70 | 15.70 | 0.06 | 0.38 | 1.22 | 1.43,1.43,1.41,1.43 | 1.43 | 0.21 | 17.21 |
| C | 15.81 | 15.86,15.83,15.84,15.85 | 15.86 | 0.05 | 0.32 | 1.13 | 1.13,1.13,1.13,1.12 | 1.13 | 0 | 0.00 |
| D | 16.09 | 16.15,16.12,16.13,16.14 | 16.14 | 0.05 | 1.81 | 1.81 | 2.05,2.07,2.06,2.07 | 2.06 | 0.25 | 13.81 |
| | | | Average | 0.05 | 0.3 | | | Average | 0.14 | 9.4 |

[a] Predicted using average input retention times obtained from duplicate experiments.
[b] Difference = experimental − predicted.
[c] % Error = [(experimental − predicted)/predicted] × 100.

the preliminary condition where neither temperature nor gradient slope had been optimized. The data from these experiments were imported into DryLab® using the LC-RP Gradient/Temperature (4 runs) mode and the DryLab® resolution map generated as shown in Fig. 6. This map represents a plot of sample resolution for various critical pairs as a function of gradient time ($t_G$) and temperature. Calculated peak resolutions of 0.16–1.22, in increments of 0.07, are shown as color coded regions and give a visual representation of the robustness of the separation. The predicted chromatogram for a temperature of 30 °C and a $t_G$ of 34 min is shown in the lower part of Fig. 6. The resolution table (shown in Fig. 7) provides an alternative display of the resolution as a function of gradient time and temperature matrix. The black-lined boundary indicates the operating space within which a reasonable separation ($R \geq 1.00$) can be obtained with critical pairs being either A&B (designated as 2, 3) or B&C (designated as 3, 4). For example, for a $t_G$ of 34 min and a temperature of 30 °C, a resolution of 1.13 is predicted for the critical pair B&C (see highlighted entry in Fig. 7). This analysis predicts an optimum separation for B&C at a gradient time of 35 min and at a temperature of 28 °C ($R = 1.21$) and an optimum separation for A&B at a gradient time of 36 min and at a temperature of 27 °C ($R = 1.24$). However, for practical reasons with respect to the effective control of the column temperature, a gradient time of 34 min and a temperature of 30 °C (condition shown by dotted line in Fig. 6) were selected as the most robust conditions from this analysis and these values were employed as the final optimized condition.

Data for the chromatographic runs 1–4 (described above) were obtained in duplicate (experiments 1 and 2 for each run) to assess the impact of minor changes in RT (in the input data) on the predictive power of DryLab®. The largest variations in input retention times for API, and components A, B, C and D were between experiments 1 and 2 of *Run 1* and ranged from 0.29 to 0.42%. Variations in retention times between experiments 1 and 2 for runs 2 through 4 were less significant and ranged from 0 to 0.16%. This was found to result in a very minor impact on the predicted DryLab® resolutions. That is, for the critical pairs API&A, A&B, and B&C, the variations in predicted resolutions were within ±0.01. The largest variation was observed in the case of components C&D, where the predicted resolutions varied by 0.08 ($R = 1.77$ versus $R = 1.85$).

### 3.6. Experimental verification of DryLab® optimized method

To verify the DryLab® prediction, an experiment was carried out using the final optimized conditions as summarized in Table 4 (column 3). The predictive ability of the gradient time-temperature model was evaluated by comparing the predicted and experimentally obtained retention times and resolutions (Table 5). The compared retention times were in excellent agreement, with the average of the errors being 0.3%. Similar levels of predictive accuracy for DryLab®, in terms of retention time, have been reported in recent studies by Corredor et al. [3] and Fekete et al. [8]. In the case of the resolutions obtained, these values were less accurately predicted by DryLab®, and had slightly higher errors (average of 9.4% in Table 5). However, this is not atypical; Fekete et al. also reported larger prediction errors in the case of Rs values (average 6.5%) compared to predicted retention time errors (average 1.9%) for a two-dimensional gradient time-mobile phase pH model (see Table 3; Ref. [8]) and, if needed, an adjustment over the plate number would be possible to improve the predictive accuracy of the model. It should be noted that the errors in resolution are the result of error propagation of four values: the retention times tR1 and tR2, and the peak widths w1 and w2, which lead to a somewhat higher value of the Rs precision [8]. The chromatograms from the DryLab® prediction and the verification experiment are shown in Fig. 8 for visual comparison.

### 3.7. Robustness evaluation

As a means of evaluating the method's robustness prior to method validation, we were particularly interested in whether DryLab® could be used to accurately predict the outcome of the robustness study. The robustness was verified by changing selected chromatographic parameters one at a time within a range of approximately ±20% of the method condition (see Table 6). The chromatographic system suitability requirement for the resolution was set as being between API and B, with a criterion of must be ≥2.0. Note that component A was not considered with respect to this requirement, as during the HPLC method development period the API manufacturing process had evolved to the point that this

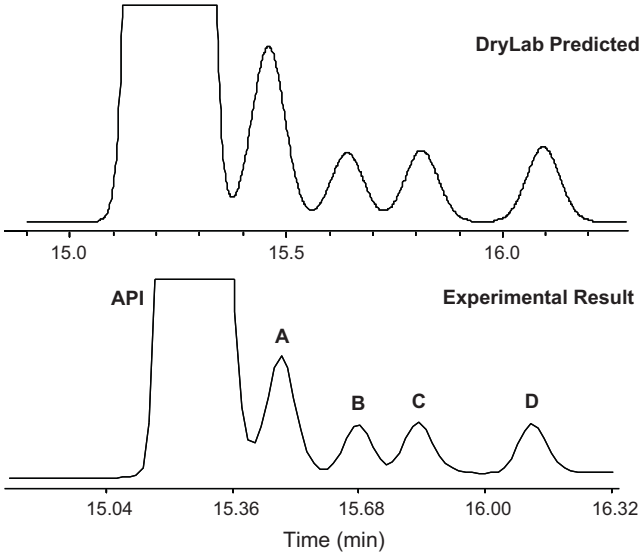


**Fig. 8.** DryLab® predicted and experimentally obtained (using DryLab® optimized separation conditions) of Dapagliflozin impurity marker components. See Table 4 for final method conditions employed.

**Table 6**
Resolution values obtained for robustness verification.

| Experiment # | Parameter varied (value) | Resolution (API and B) | | | |
|---|---|---|---|---|---|
| | | DryLab predicted | Experimental | % Difference (method robustness) | % Error (predictive accuracy) |
| 1 | Initial %B (10%) | 2.96 | 3.28 | 2.8 | 10.81 |
| 2 | Initial %B (20%) | 3.17 | 3.10 | −2.8 | −2.21 |
| 3 | Column temperature (25 °C) | 2.88 | 3.15 | −1.3 | 9.38 |
| 4 | Column temperature (35 °C) | 3.25 | 3.19 | 0.0 | −1.85 |
| 5 | Flow rate (0.8 mL min$^{-1}$) | 2.87 | 3.11 | −2.5 | 8.36 |
| 6 | Flow rate (1.2 mL min$^{-1}$) | 3.17 | 3.24 | 1.6 | 2.21 |
| 7 | TFA content (0.025%) | NA | 3.20 | 0.3 | NA |
| 8 | TFA content (0.075%) | NA | 3.21 | 0.6 | NA |
| 9 | Wavelength (216 nm) | NA | 3.20 | 0.3 | NA |
| 10 | Wavelength (224 nm) | NA | 3.20 | 0.3 | NA |
| 11 | Actual method condition[a] | 3.06 | 3.19 | NA | 4.25 |

% Error = [(experimental − predicted)/predicted] × 100, used to assess predictive accuracy of DryLab®.
% Difference = [($R_{exp} - R_{amc}$)/$R_{amc}$] × 100, used to assess method robustness, where $R_{exp}$ is the experimental resolution obtained at any varied condition and $R_{amc}$ is the resolution obtained under the actual method condition.
[a] 15% initial B, 30 °C, 1 mL min$^{-1}$, 0.05%TFA and 220 nm.

**Table 7**
Analytical figures of merit for validation of optimized method.

| Analytical figures of merit | | | |
|---|---|---|---|
| Test | Acceptance criteria | Result | |
| Specificity | Resolve critical impurities ($n$ = 4) | Resolution of impurities achieved | Pass |
| Linearity[a] | $R$ squared must exceed 0.995 | $R$ squared = 0.9992 | Pass |
| Precision (sample repeatability) | RSD ≤ 2.0% | RSD = 0.40% ($n$ = 6) | Pass |
| Precision (injection repeatability) | RSD ≤ 2.0% | RSD = 0.30% ($n$ = 10) | Pass |
| Precision (intermediate[b]) | RSD ≤ 2.0% | RSD ≤ 0.79% | Pass |
| Sensitivity (impurities, $n$ = 4) | RSD ≤ 15.0% | RSD ≤ 6.47% | |
| | | QL ≤ 0.03% | |
| | | DL ≤ 0.01% | Pass |

[a] Range from 70% to 130% of the working concentration.
[b] Analyze samples from three batches on three days.

impurity was no longer being generated at detectable levels. The other acceptance criterion was that for the API tailing factor, which was set at ≥0.8 and ≤1.5. DryLab® was used to predict the resolutions (between API and B) for all the conditions studied and these values were compared with the experimental results. These results are also shown in Table 6. The experimental resolution values are all consistently above 3, and significantly exceed the required value of Rs ≥2. The % difference deviations in resolution between the deliberate change and the actual method condition, which reflect the robustness of the method, are all within an acceptable range (−2.5 to 2.8%), indicating that the method would be considered robust. The DryLab® predicted values for the resolution between API and B are all in good agreement with the experimental values, with the average error being 5.6% over the 7 measurements shown in Table 6. These results show that computer simulation in DryLab® can be used with reasonable accuracy to predict the outcome of such robustness studies. With respect to the USP tailing factor, this ranged from 1.00 to 1.02 for all the conditions studied, which is well within the acceptable range of 0.8–1.5.

### 3.8. Validation of final optimized method

In compliance with USP <1225> [18], ICH Q2B [19], and Analytical Procedures and Methods Validation, FDA draft guidance August 2000 [20], the method was validated for the following parameters: method specificity, method suitability as a stability indication assay, linearity for assay, injection repeatability, sample repeatability, intermediate precision, linearity of impurities, accuracy of impurities, sensitivity of impurities, stability of working standard and sample solutions, robustness of sample extraction, and robustness of the method to withstand deliberate changes in the chromatographic conditions. Table 7 provides the analytical figures of merit for the validation of the method. In addition to the tests, the acceptance criteria are also provided. These acceptance criteria were established in the validation protocol prior to starting the validation. The results are all within the acceptance criteria. Based on a well designed method development strategy, the robustness of the method is insured and the validation becomes a simple exercise which demonstrates the method is suitable for its intended purpose.

### 3.9. Advantages of final optimized method

The intended purpose of this method is the assay and impurity profiling of API. Compared to the initial method, the final optimized method has the following advantages: all impurities have now been successfully resolved from each other and from the API, whereas the initial method could not separate the API/A pair, or B/C pair, the run time has been reduced by 18%, that is, from 55 min to 45 min, and finally the tailing factor for the API has not been compromised (now 1.02 versus 1.03 originally). Also, we now have a full understanding of the design space in terms of the organic modifier, the separation temperature, and the gradient steepness effects. The finalized method addresses all the predefined conditions and has been successfully validated. Currently the method is utilized to determine the impurity profile of the API batches.

## 4. Conclusions

This paper describes the application of a rational HPLC method development strategy to solve a challenging problem, namely, the development of a reversed phase method to separate the components of a complex pharmaceutical sample containing several structurally very similar API process impurities. The first step in

solving this problem was addressed by conventional automated column screening, which significantly reduces the time involved in choosing a specific column chemistry. However, instead of selecting the software starting conditions based solely on these column screening results, a stepwise strategy allows the design space for final optimization to be better defined by further evaluating the separate influences of organic modifier and temperature on the chromatographic separation. In this case, the final DryLab® optimization, which included gradient time and percent organic as critical parameters, generated predictions that were verified experimentally with a high degree of accuracy. This approach is not only beneficial in achieving a more robust method, but it also allows more solvent and temperature conditions to be initially explored to achieve the required selectivity. Clearly, if an understanding of the influence of certain critical parameters is developed at an earlier stage, then limits can be placed during the software optimization; rather than employing a time consuming brute-force approach. Finally the robustness of the method was also simulated using DryLab® and examined experimentally. In this case, the DryLab® predicted values for the resolution between the API and its bromo-analog (B) were all in good agreement with the experimental values. These results, and the other validation results, demonstrate that the method is appropriate for its intended use. Note that, the other validation parameters have been included for completeness only; once the robustness was established by the DryLab® predictions the remainder of the subsequent verification by experiment becomes a simple reiterative exercise. This is a significant, although subtle, difference between our strategy and that of previous researchers (3, 4). This study also demonstrates that factors such as column chemistry, type of organic modifiers and separation temperature can have a profound and oftentimes interrelated effect on the chromatographic separation of isomers, bromo analogs and other structurally very similar impurities. Therefore, it is critical to adopt a rational strategy, as demonstrated here, to evaluate the interplay of these factors, thereby greatly enhancing method development efficiency.

## Acknowledgement

The authors would like to thank Ms. Merrill L. Davies (Research and Development, Bristol Myers Squibb Co.) for her help in generating the MeDuSA data.

## References

[1] T. Baczek, Curr. Pharm. Anal. 4 (2008) 151.
[2] K.P. Xiao, Y. Xiong, F.Z. Liu, A.M. Rustum, J. Chromatogr. A 7 (2007) 1.
[3] R.M. Krisko, K. McLaughlin, M.J. Koenigbauer, C.E. Lunte, J. Chromatogr. A 1122 (2006) 186.
[4] C.C. Corredor, J.A. Castoro, J. Young, J. Pharm. Innov. 4 (2009) 121.
[5] I. Molnar, J. Chromatogr. A 965 (2002) 175.
[6] J.W. Dolan, L.R. Snyder, N.M. Djordjevic, D.W. Hill, T.J. Waeghe, J. Chromatogr. A 857 (1999) 21.
[7] J.W. Dolan, L.R. Snyder, R.G. Wolcott, P. Haber, T. Baczek, R. Kaliszan, L.C. Sander, J. Chromatogr. A 857 (1999) 41.
[8] S. Fekete, J. Fekete, I. Molnar, K. Ganzler, J. Chromatogr. A 1216 (2009) 7816.
[9] E.F. Hewitt, P. Lukulay, S. Galushko, J. Chromatogr. A 24 (2006) 1.
[10] T.H. Hoang, D. Cuerrier, S.M. McClintock, J. Chromatogr. A 991 (2003) 281.
[11] W. Li, H.T. Rasmussen, J. Chromatogr. A 24 (2003) 165.
[12] B.D. Karcher, M.L. Davies, E.J. Delaney, J. Clin. Lab. Med. 27 (2007) 93.
[13] P. Cole, M. Vicente, R. Castañer, Drugs Future 33 (2008) 745.
[14] http://www.usp.org/USPNF/columnsPQRIapproach.html (accessed 26.08.10).
[15] B. Bidlingmeyer, et al., Pharmocopeial Forum 31 (2) (2005) 637.
[16] L.R. Snyder, J.W. Dolan, P.W. Carr, J. Chromatogr. A 1060 (2004) 77.
[17] L.R. Snyder, J.J. Kirkland, J.W. Dolan, Introduction to Modern Liquid Chromatography, 3rd ed., John Wiley and Sons Ltd., Hobroken, NJ, 2010, p. 270.
[18] http://www.pharmacopeia.cn/v29240/usp29nf24s0_c1225.html.
[19] http://www.ich.org/cache/compo/363-272-1.html#Q2A.
[20] http://www.fda.gov/downloads/Drugs/GuidanceComplianceRegulatoryInformation/Guidances/ucm122858.pdf.